Nuclear Materials Authority
P.O.Box 530 Maadi, Cairo, Egypt

ISSN 2314-5609
Nuclear Sciences Scientific Journal
10, 1-24
2021
http://www.ssnma.com

GEOLOGICAL AND MINERALOGICAL STUDIES OF U-Th-BEARING PEGMATITES AT GABAL SUWAIR AND GABAL KHOSH DABA AREA, SAINT CATHERINE, SOUTH CENTRAL SINAI, EGYPT

MAHMOUD M. NASR
Nuclear Materials Authority, P.O. Box 530, Maadi, Cairo, Egypt

ABSTRACT

The pegmatites of Gabal Suwair and Gabal Khosh Daba area are situated in the north of St. Katherine city, South-Central Sinai. The studied pegmatites considered to be the youngest outcropped rocks following the arc granitoids and the post-collision granites. They show numerous radioactive anomalies along different zones in the studied area and spatially belong to the zoned and unzoned both types of pegmatites. The radiometric investigations of the anomalous pegmatite show that their maximum equivalent uranium content (eU) is reaching up to 670 ppm while their eTh is reaching up 180 ppm at Gabal Khosh Daba pegmatites. While the maximum eU and eTh contents at Gabal Suwair pegmatite are 520 and 330 ppm respectively. The integrated mineralogical studies revealed the occurrence of uranium minerals (i.e. uraninite, brannerite and carnotite) as discrete large crystals in the zoned pegmatites; while the unzoned ones enclosed samarskite, betafite, tanteuxenite, uranothorite and thorianite. The presence of uraninite (primary mineral) at the zoned pegmatite suggest their syngenetically origin during magmatic processes, while, the secondary uranium minerals presented in the unzoned pegmatite as fissure filling are most probably related to the hydrothermal activity. Accordingly, the studied widespread mineralized pegmatite could be a promising area for uranium and thorium exploration and evaluation.

INTRODUCTION

Several studies worldwide have revealed the presence of granite-pegmatite-hosted uranium and thorium (e.g. Matsubara et al., 1995; Erict, 2005; William et al., 2006 and Pal et al., 2007). Rare-metal pegmatites mineralization can be attributed either to magmatic or post-magmatic metasomatic processes (Schwartz, 1992; Abdalla et al., 1998; Raslan and Ali, 2011 and Ali et al., 2021). Pegmatites occur as sharply bounded homogeneous to zoned bodies within igneous or metamorphic host rocks (Černý and Ercit 2005).

Older granites include rocks referred to grey granites by Hume (1935), old (grey) granites by El-Ramly and Akaad (1960), synorogenic plutons by El-Shazly (1964), older granites by Akaad and Noweir (1980) and as (G-1) granites by Hussein et al., (1982) and pertain to Cordillerian stage in the classification of El-Gaby et al. (1988). The younger granite (monzogranite and syenogranite) is the most dominant rock unit exposed in the study area were referred to as Gattarian granites (Hume, 1935), younger granites (El-Ramly and Akaad, 1960), late-to

post-orogenic granites (El-Gaby, 1975).

Many radioactive occurrences have been recorded along different localities of the Saint Catherine area and south-Central Sinai. However, the radioactive mineralization is mainly restricted to the granite pegmatite bodies associated with the monzogranite and syenogranite rocks. The geology and radioactivity of the areas were studied by many authors (Barron, 1907; El-Shazly et al. 1974; Eyal 1975; El-Ghawaby 1984; El-Sheshtawy, 1984; Ibrahim, 1991, Bishr 2007; Raslan and Ali, 2011; Raslan, 2015 and Sallam et al., 2019).

U-Th-bearing pegmatites in Saint Catherine area still need to be described properly, in order to assess their economic potential. This work aims to present constraints on radioactive mineralization associated with different lithological pegmatites types based on detailed geological and mineralogical investigations at Gabal Suwair and Gabal Khosh Daba area.

GEOLOGIC SETTING

The studied area is bounded by lat. 28° 37’ 09” – 28° 39’17” N and long. 34° 01’ 02” – 34° 05’ 44” E (Fig.1). The basement exposures comprises older (arc granitoids) to younger (post-collision) granitoids that dissected by dyke swarms with NE-SW and NW-SE trends. The older granitoids are mainly represented by granodiorite. They are exposed at the north to central parts of the mapped area and covering of about 25% (Fig. 1). They appear as medium- to coarse-grained, hard and massive, dark grey in color, strongly jointed, highly fractured and display strong exfoliation weathering containing mafic xenoliths of different shapes and sizes.

On the other hand, the younger granites are mainly of monzogranite and syenogranite in composition. They cover about 70% of the mapped are especially along the eastern

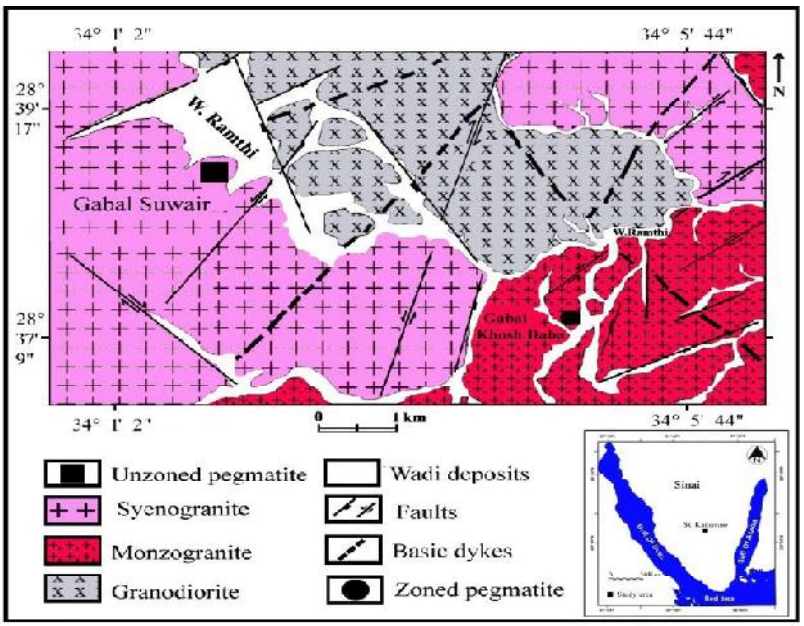

Fig.1: Geologic map of Gabal Suwair and Gabal Khosh Daba area, Saint Catherine, South Central Sinai, Egypt (map constructed by author).

and western part. Monzogranite show high relief mountains features and intruded into granodiorite with sharp contacts (Fig. 2). Also, small offshoots and veinlets are extended from the monzogranite into the surrounding granodiorite to suggest its forceful emplacement. Generally, they are of medium- to coarse-grained with pinkish white colors and highly jointed. The rocks show moderate to high degree of weathering and dissected by numerous dykes with predominant NE-SW and NW-SE trends and contain pegmatite bodies of different composition and attitudes. The syenogranite rocks show significant high relief mountains, and intruded into the monzogranite with sharp contacts (Fig. 3). These rocks are hard, massive and medium to coarse-grained with reddish pink colors. They are extensively fractured, highly jointed and weathered. Exfoliation and minor cavities are recognized; also, weathered cavities with different sizes are observed with rounded to subrounded shapes. They are dissected by basaltic dykes and aplitic-pegmatitic veins (Figs. 4 & 5).

The unzoned pegmatite hosted in syenogranite of Gabal Suwair and occurring as large elongated bodies and veins, dykes and small pockets as well as lenses with dimensions ranging from 2 to 10 meter in width hosted in syenogranite of Gabal

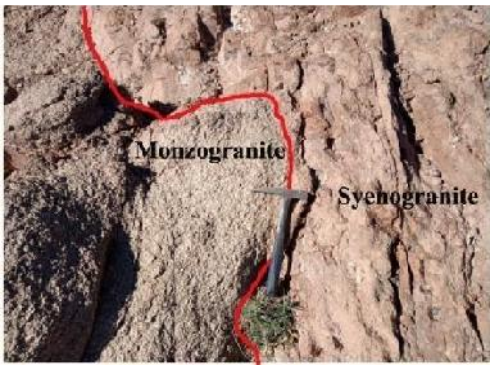

Fig.3: Photograph shows sharp contacts between monzogranite and syenogranite

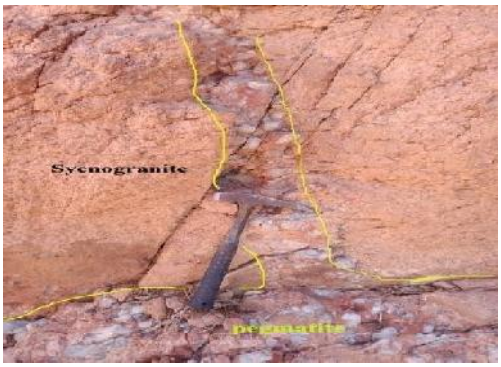

Fig.4: Photograph shows syenogranite dissected by aplitic-pegmatitic veins

Fig.2: Photograph shows sharp contacts between granodiorite and monzogranite.

Fig.5: Photograph shows syenogranite dissected by pegmatitic veins in Gabal Suwair

Suwair. The pegmatitic dykes have thickness vary from 30 to 70 cm and extend for about 25m. They exhibit variation in color and display sharp contacts with their granitoid host. Mostly, the pegmatites are composed of K-feldspar at the margins followed by quartz at the core. Quartz occurs as very coarse crystals of different colors such as rose, milky white or even colorless. They are dissected by numerous fractures completely stained by iron oxides and associated with radioactive minerals (Figs. 6&7).

The studied zoned pegmatites hosted by monzogranite in the eastern area of Gabal Khosh Daba are vary between large to small pockets and are very coarse grained (Fig.8). They are ranging between 2 to 5 m in width and from 10 to 50 m in length showing its significant zoned characteristics. Their zoned criteria display border zone, wall zone (coarse-grained granites), intermediate zone (K-feldspars) and core zone (quartz).

The border zone is composed mainly of aplitic-pegmatitic, while the wall zone has the same fabric of the host rocks but with coarser-grained and darker color due to more mafic content, the contact with the monzogranite host rock is always gradational. The wall zone is mainly composed of plagioclase, K-feldspars and quartz. The intermediate zone is marked by its sharp contact with the wall zone and composed of mega crystals of K-feldspar which represent the common crystal components with considerable amounts of plagioclase, quartz, biotite and muscovite. The core zone is essentially composed of massive quartz and has sharp contact with the intermediate zone (Fig. 9).

Fig.6: Photograph shows unzoned pegmatite dissected by numerous fractures of Gabal Suwair.

Fig.7: Photograph shows pegmatite veins in syenogranite with fractures stained by iron oxides.

Fig.8: Field photograph showing zoned pegmatite of Gabal Khosh Daba

MATERIALS AND METHODS

The field radiometric survey carried out using car-borne gamma spectrometric technique, which can allow to pick up more than

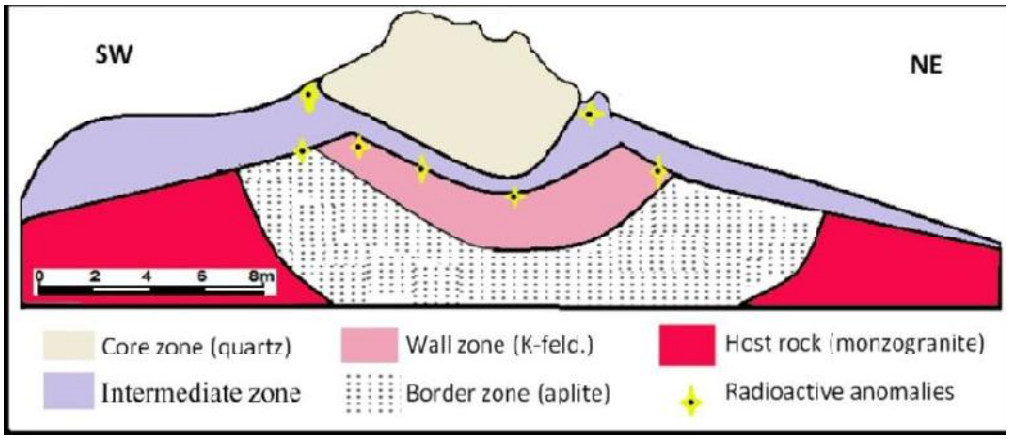

Fig. 9: Sketch of the zonal distribution of the pegmatite body of Gabal Khosh Daba

85% of the radioactive emission concerning the upper 15 to 30 centimeters of ground (1 meter maximum) (Ulvsand et al., 2002 and Gaafar et al., 2014).

The car-borne multichannel gamma-ray spectrometric system Model GR-660 is composed of a GR-320 of portable multichannel gamma-ray spectrometer and a large volume scintillation detector. The location for each measurement point is determined by the GPS instrument.

Moreover, a detailed ground gamma-ray spectrometric survey was carried out at the studied area using the Rs-230 BGO- Super-spectrometer portable multichannel gamma-ray spectrometer.

The petrography and photomicrographs were carried out using a Nikon (Optiphot-Pol) polarizing microscope equipped with a full automatic photomicrograph attachment (Micro flex AFX-II). Twenty samples were collected from the studied granitic rocks and pegmatite bodies in order to study the petrography and mineralogy. Nineteen thin sections were prepared and studied to determine the petrographic characteristics of these rocks.

The radioactive samples were crushed, ground, and sieved before subjecting the liberated size fractions to heavy-mineral separation, using bromoform (specific gravity = 2.85 g/cm3). The heavy mineral grains were manually picked from each of the obtained heavy fractions under binocular microscope. Some of these selectively picked grains were analyzed by X-ray diffraction technique (XRD), using Philips X-ray generator model PW 3710/31 a diffractometer with automatic sample changer model PW1775. The X-ray radiation used is Cu-target tube and Ni filter at 40 kV and 30 mA. This instrument is connected to a computer system using X-40 diffraction program and ASTM cards for mineral identification. The metamict state is characterized by structure disorder (amorphous to X-rays) while the crystal habit is frequently well developed. The essential features of this state were discussed by Pabst (1952). The metamict state was changed by appropriate heating at temperatures higher than 800°C leading to their recrystallization.

Also, some of the separated grains were examined by Environmental Scanning Electron Microscope (SEM), Philips XL 30 with energy-dispersive X-ray (EDX) unit. The applied analytical conditions were an accelerating voltage of 30 kV with a beam diameter of 1µm for a counting time of 60-120 s and a minimum detectable weight

concentration ranging from 0.1 wt % to 1wt %. These analyses were carried out at the laboratories of the Egyptian Nuclear Materials Authority (NMA).

RESULTS

Petrography

The petrographic description of the granitic rocks was made based on QAP (Streckeisen, 1976) modal mineralogical composition, they are classified as granodiorite, monzogranite and syenogranite (Fig. 10).

Granodiorite is mainly composed of plagioclase, quartz, K-feldspar, hornblende and biotite. Zircon, apatite and opaques are the accessories (Figs.11& 12). Plagioclase exhibits subhedral tabular crystals with pericline twinning. Potassic feldspar present as subhedral crystals, and showing simple twinning and corroded by quartz. Hornblende forms large subhedral crystals of green color and moderate pleochroism phenomenon from green to brownish-green. It exhibits pericline twinning and two sets of cleavages. Biotite exhibits subhedral to anhedral flaks of brownish color. Hornblende and biotite are altered to secondary mineral of chlorite. The accessory minerals are represented mainly by zircon, titanite and opaques.

Monzogranite show equigranular and hypidiomorphic textures and mainly composed of quartz, K-feldspar, plagioclase and flakes of biotite (Figs.13& 14). Quartz content ranges from 32.95 to 40.40 % in the studied thin sections, it occurs as subhedral to anhedral crystals filling the spaces between other constituents. Potash feldspar (25.40 to 32.50%) represented by orthoclase perthite, orthoclase and microcline perthite. The orthoclase-microperthite exhibits a characteristic simple twinning. Plagioclase (24.50 to 27.90%) with oligoclase composition (An_{18-33}) commonly exhibit albite twin lamellae, albite-Carlsbad and rarely pericline twinning. Biotite occurs as euhedral to subhedral flaky crystals with brownish color. Zircon, apatite, titanite and opaques are the

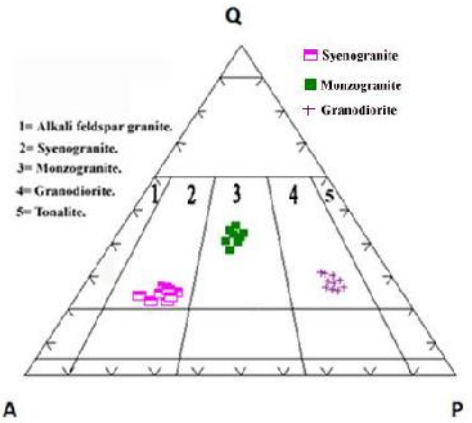

Fig.10: QAP modal classification and nomenclature of the studied granite rocks (Streckeisen, 1976)

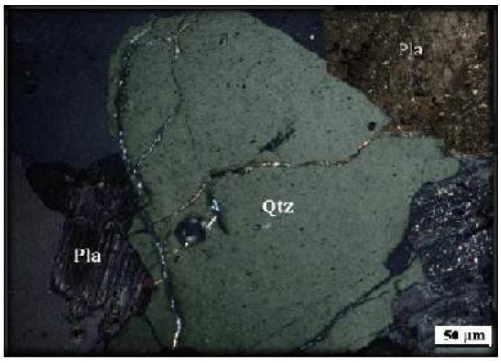

Fig.11: Photomicrograph shows the components of granodiorite (plagioclase (pla), quartz (Qtz) minerals

accessories. Secondary minerals are the least dominant mineral constituents represented by chlorite, secondary muscovite, sericite and epidote.

Syenogranite show hypidiomorphic granular texture and consist mainly of alkali feldspar (51.3 to55.8%), quartz (21.0 to25.0%), plagioclase (17.0 to21.8%) as patchy type orthoclase micro-perthite crystals (Fig.15). Accessories are zircon, apatite and opaques. Sericite, kaolinite, muscovite, chlorite

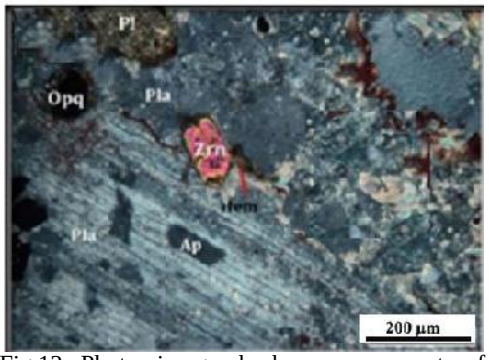

Fig.12: Photomicrograph shows components of granodiorite (plagioclase (pla), quartz , K-feldspar, Zircon (Zrn) and apatite (Ap) minerals

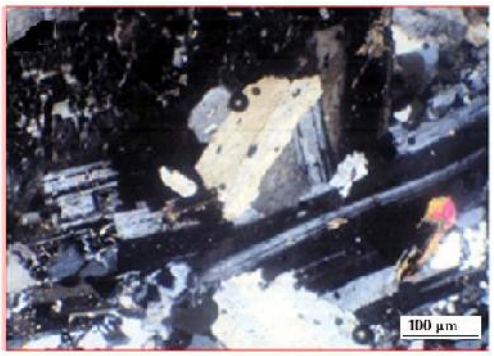

Fig.15: Photomicrograph shows the comopnent of syenogranite; K-feldspar, quartz, plagioclase. biotite flakes and zircon

Fig.13: Photomicrograph shows the components of monzogranite; quartz (Qtz), K-feldspar

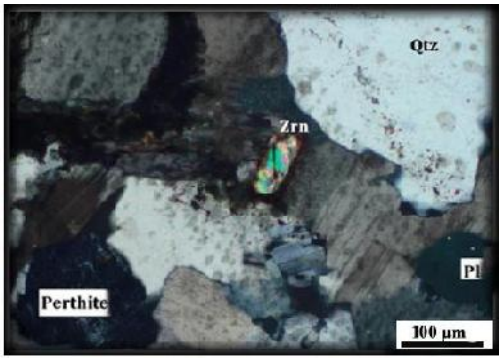

Fig.14: Photomicrograph shows the components of monzogranite; quartz (Qtz), K-feldspar (Perthite) , plagioclase (pl) and zircon (Zrn).

and epidote represent secondary alteration minerals. Biotite appears as yellowish brown grains (Fig.16) contains many accessory minerals as zircon, while opaques are present in lower amount with some samples appear to be barren of mafics.

Petrographically, the studied pegmatite bodies are holocrystalline, coarse to very coarse grained and composed mainly of quartz, K-feldspars, plagioclase and mica, the accessory minerals are mainly zircon, apatite and opaques (Figs. 17 & 18).

Quartz is the most predominant mineral (30.0 to 38.3 %), found as subhedral to euhedral interstitial grains between plagioclase and perthites. K-feldspars (27.1 to 34.2%) represented by orthoclase, microcline and microcline perthite. Perthite and antiperthite are subhedral to euhedral prismatic megacrystal corroded by quartz. Plagioclase (An_{15-28}) albite to oligoclase in composition occurs as euhedral to subhedral crystals exhibiting slight deformation; sericitization and muscovitization in some plates. Plagioclase contents ranges from 19.3 to 22.40 % in the studied thin sections. Mica occurs as subhedral to euhedral flakes of muscovite intercalated between feldspars and quartz intimately associated with accessory mineral.

The wall zone has the same composition

of the host rock with rich in iron oxides. The intermediate zone of the studied pegmatite consists essentially of distinctly large crystals of orthoclase and microcline perthite, quartz, plagioclase and biotite. Zircon occurs as colorless subhedral to euhedral prismatic crystals generally enclosed in mica and plagioclase. These crystals surrounded by pleochroic haloes due to the alpha decay of uranium and or/thorium contents, which cause the damage of the crystal lattice of zircon (metamictism phenomenon).

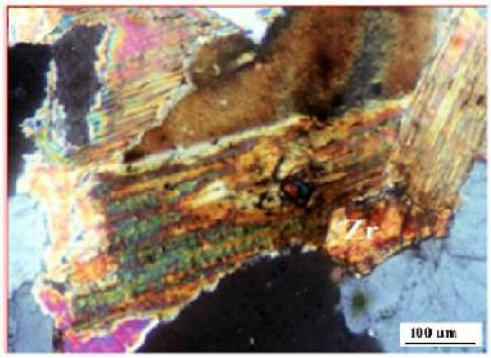

Fig.16: Photomicrograph shows the biotite flakes and zircon (Zr) of syenogranite

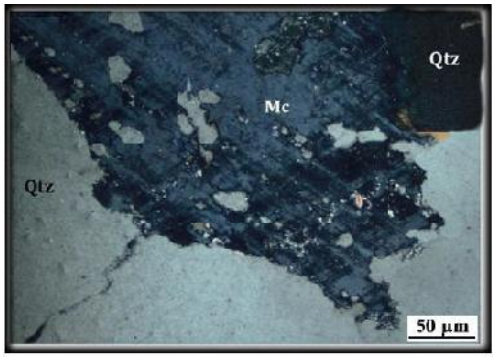

Fig.17: Photomicrograph shows the main components of pegmatite rocks; quartz (Qtz), K-feldspar (Mc) and plagioclase

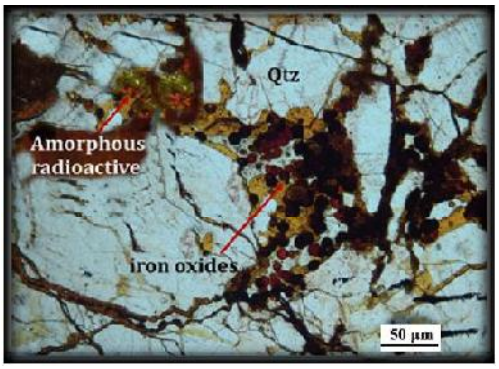

Fig.18: Photomicrograph showing radioactive minerals as fracture and fissure filling of pegmatite rocks

Radioactivity

Gamma-ray spectrometry survey is proposed to provide quantitative determination of radioelement (uranium, thorium and potassium) content in the granitoids and pegmatites. Carborne and hand-held spectrometry survey along well geologic inspection, supported by GPS location, will be carried out along the selected profiles. The spectrometric surveys used to determine the radioactive background for the different rocks in the studied area and constructed radioactive map anomalies.

The radiometric studies of the anomalous pegmatite samples show that their equivalent uranium contents (eU) up to 670 ppm while their equivalent thorium (eTh) 180 ppm in Gabal Khosh Daba and display 520 ppm (eU) and 330 ppm (eTh) in Gabal Suwair. The carborne survey on the contrary rocks of the granites eU and eTh contents range from 2 to 22 and from 4 to 90 ppm respectively. This indicates strong post magmatic uranium enrichment in the pegmatitic melt.

The average eU/eTh ratio is 2.9 in zoned pegmatite (Table 1) and average eU/eTh ratio 0.5 in host granitic rocks. However the average eU/eTh ratio is 1.7 in unzoned pegmatite while average eU/eTh ratio 0.4 in host granitic rocks that means a secondary enrichment of

Table 1: Summary of the measurements eU, eTh, K and eU/eTh data of the studied pegmatites

Type	Parameter	eU (ppm)	eTh (ppm)	K (%)	Pegmatite eU/eTh
Zoned G. Khosh Daba	Minimum	20	30	3.1	0.66
	Mean	200	70	2.1	2.9
	Maximum:	670	180	9.2	3.7
Unzoned G. Suwair	Minimum	30	15	2.2	2
	Mean	250	150	1.7	1.7
	Maximum:	520	330	7.4	1.6

uranium over thorium. The high eU/eTh ratio is due to the presence of uranium bearing accessories carried by hydrothermal solutions from the relatively deep-seated and were precipitated along fissures and fault plans within the pegmatites.

The carborne maps (spectrometric maps using car-borne multichannel gamma-ray spectrometric system composed of portable multichannel gamma-ray spectrometer and a large volume scintillation detector) display that the relative high uranium contents are represented by an elongated and circular anomaly zone recorded in the southwestern parts of the mapped area (Fig.19). The highest eTh values are mainly observed at northeastern and southern parts of the mapped area (Fig.20). Potassium content varying from 0.3 % to 7.3 % and the highest

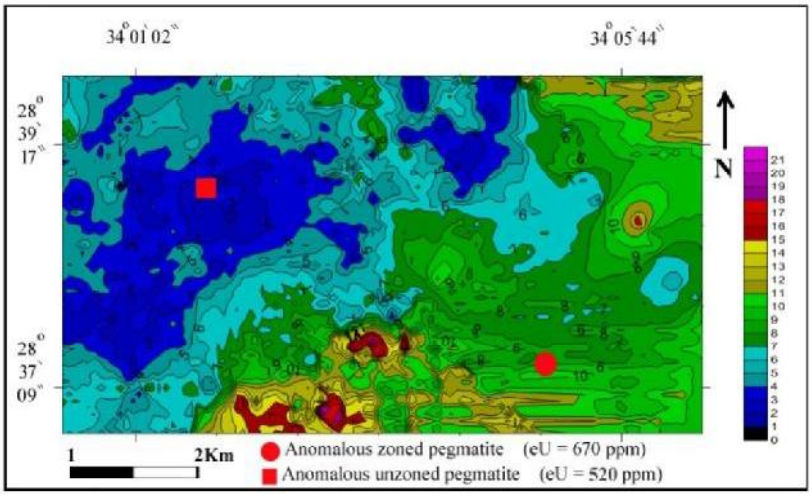

Fig. 19: Contour map shows eU anomalies at the study area

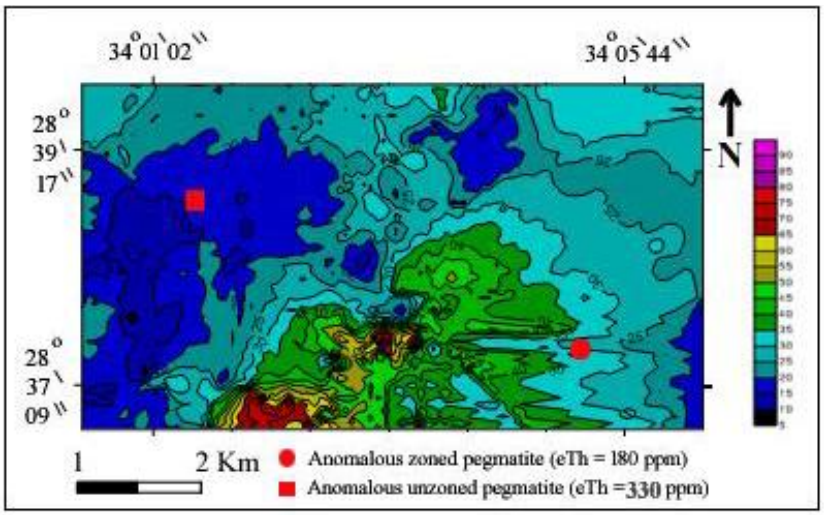

Fig. 20: Contour map shows eTh anomalies at the study area

values are located at the eastern and central parts of the mapped area (Fig.21).

Mineralogy

The detailed mineralogical investigation along numerous radiometric anomalies related to pegmatitic bodies, zoned and unzoned types, revealed the presence of several uranium minerals. The X-ray diffraction (XRD) and environmental scanning electron microscope (ESEM) studies on the anomalous samples indicate the presence of essential uranium minerals, thorium-uranium minerals and niobium-tantalum minerals, while, zircon and copper minerals occurs as accessory and gangue minerals. The identification of some uranium mineral by XRD technique are detected after heating treatment due to the minerals were metamict and required heating to develop crystallinity. So, the uranium minerals were subjected to heating samples separated from air to 800°C for three hours.

Uranium minerals

Uraninite (UO_2)

Uraninite is the main primary uranium mineral present in the zoned pegmatite of Khosh Daba area. It occurs as fine anhedral crystals with black color and concoidal fractures associated with other uranium minerals in the highest radioactive measurements through the pegmatite zones. Picked crystals were carried out for X-ray diffraction investigation, which revealed the metamectization of the grains by the amorphous diffraction pattern. The XRD pattern of the heated samples illuminates the matched data of card No 5-550 for uraninite (UO_2) associated with hematite mineral (Fig. 22). The ESEM (EDX) analysis and BSE image (Fig.23) was used to characterize the chemical composition of uraninite. The EDX analysis results indicate that the crystals contain a variable content of uranium percent that fluctuated between 85.0% and 94.6% in different samples.

Brannerite ($(U,Ca,Ce)(Ti,Fe)_2O_6$)

It occurs as brown to black anhedral to subhedral crystals, in the radioactive zoned pegmatite anomaly of Khosh Daba area associated with uraninite and hematite minerals. Brannerite mineral is translucent and has a reddish brown color across the edges. The identification of brannerite mineral by XRD pattern (Fig.24) is detected after

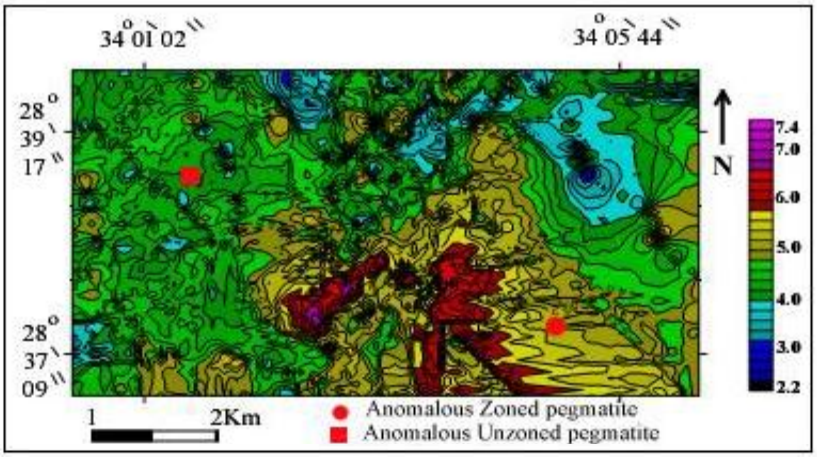

Fig. 21: Contour map shows K% at the study area

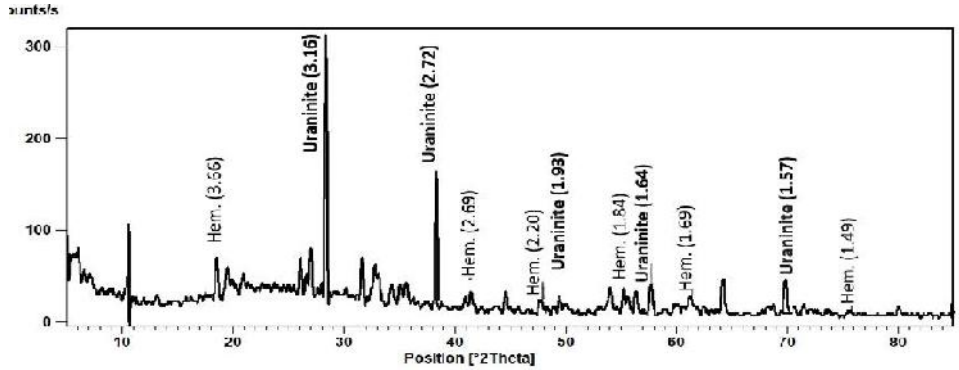

Fig. 22. X-Ray diffractogram pattern of uraninite (ASTM card No. 5-550), associated with hematite ASTM card No. (6-502) of Khosh Daba zoned pegmatite

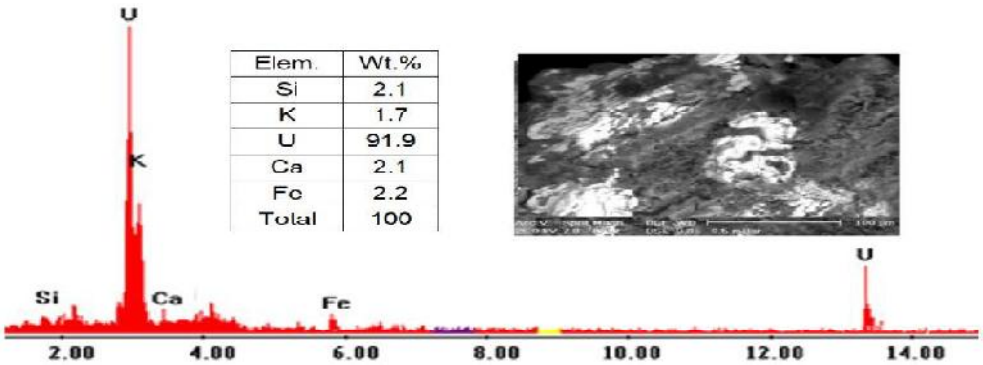

Elem.	Wt.%
Si	2.1
K	1.7
U	91.9
Ca	2.1
Fe	2.2
Total	100

Fig. 23: BSE image and EDX analysis of the uraninite mineral of the studied samples of Khosh Daba zoned pegmatite

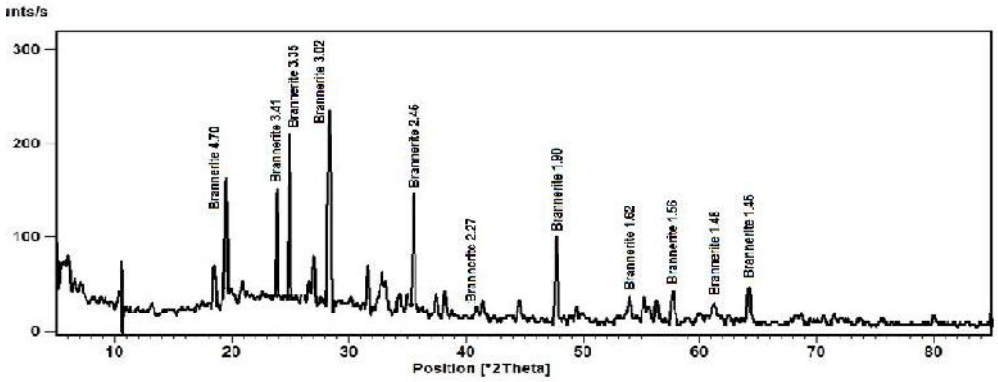

Fig. 24. XRD pattern of brannerite ASTM card No. (12-477) of the studied samples of Khosh Daba zoned pegmatite

heating due to brannerite is usually metamict and requires heating to develop crystallinity. Based on Smith (1984) brannerite is the third most important reduced uranium mineral and occurs in many different types of deposits. Although brannerite has been found in pegmatites, hydrothermal and sedimentary deposits, it is always associated with uraninite and probably forms through reactions with uraninite and titanium phases.

The elemental composition of the brannerite grains which analyzed by ESEM technique (Fig.25) shows that the highest composition are Ti, U, Nb and some U is oxidized and replaced by Ca and Nb, while the Fe partially replaces Ti. Smith (1984) concluded that, brannerite is nominally UTi_2O_6, but the U may be partially oxidized and partially replaced by Ca and rare earths. Fe may replace some of the Ti and partial hydration may occur and the formula of brannerite may be $(U,Ca,REE)(Ti,Fe)_2O_{6-8}(OH)_x$.

Mock and Ohmoto (1997) concluded that the uraninites are associated with brannerite, rutiles and ilmenite grains of the Elliot Lake District, such associations may indicate these minerals formed by hydrothermal fluids.

Carnotite [$K_2(UO_2)_2(VO_4)_2 \cdot 3H_2O$]

Carnotite occurs as opaque aggregates with greenish (canary) yellow colors as thin films in vugs and fissures in the zones of high radioactivity suggests its formation by the action of the fluid migration on the presence of uranyl and vanadate ions.

The XRD diffractogram of carnotite associated with hematite is shown on Fig.(26). The ESEM with EDX analysis shows that the V and K contents are directly proportional with the high U-contents (Fig. 27) in addition some traces of Al, Ca, Ti, Si and Fe are present.

Thorium-uranium minerals

Thorianite (Th,U)O_2

Thorianite occurs as anhedral to subhedral fine crystals of black, dark gray and submetallic to metallic luster in Gabal Suwair. The X-ray diffractogram of the selected crystals (Fig. 28) shows the matches pattern of thorianite (card No. 4-556). On the other hand, thorianite appear as small inclusions associated with uranium minerals that displayed in backscattered Scanning Electron Microscopy image and analysis (Fig. 29).

Uranothorite ((Th,U)SiO_4)

It occurs as tetragonal metamict crystals in samples of Gabal Suwair radioactive pegmatite. Uranothorite appears as dark brown with adamantine luster and commonly occurs as overgrowths on zircon crystals that reflect the sufficiently of Th-rich hydrothermal

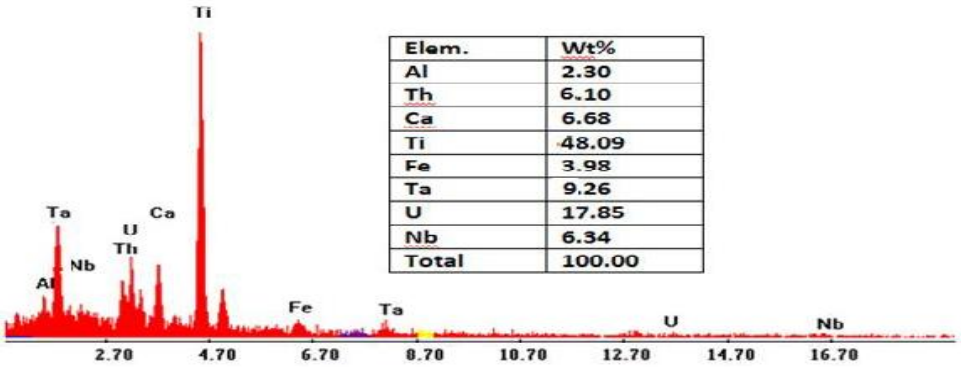

Elem.	Wt%
Al	2.30
Th	6.10
Ca	6.68
Ti	48.09
Fe	3.98
Ta	9.26
U	17.85
Nb	6.34
Total	100.00

Fig. 25: EDX analysis of brannerite mineral of the studied samples of Khosh Daba zoned pegmatite

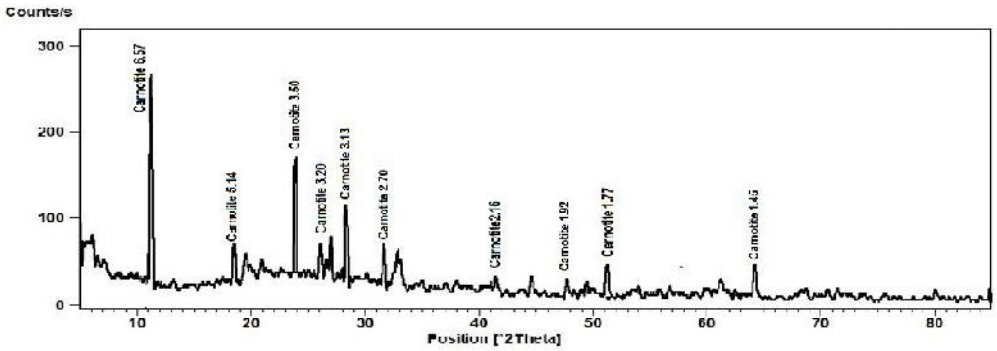

Fig. 26: X-ray diffractogram pattern of carnotite minerals ASTM card No. (8-0317)

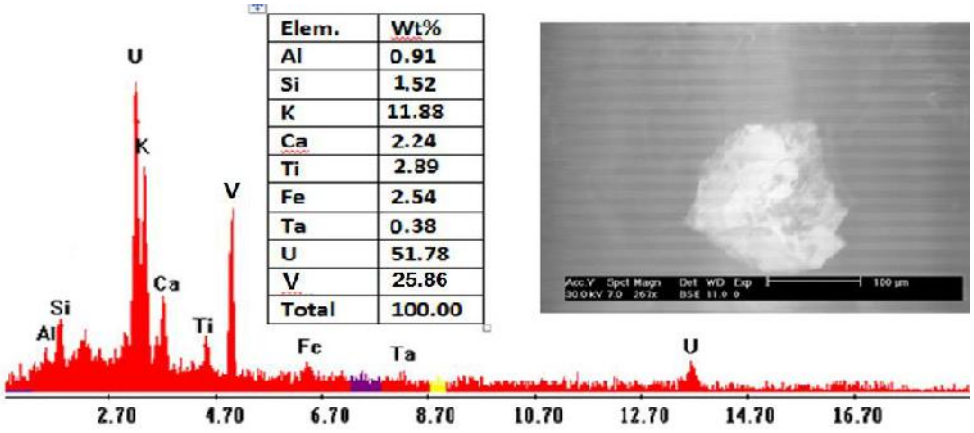

Elem.	Wt%
Al	0.91
Si	1.52
K	11.88
Ca	2.24
Ti	2.89
Fe	2.54
Ta	0.38
U	51.78
V	25.86
Total	100.00

Fig. 27: BSE image and EDX analysis of carnotite mineral

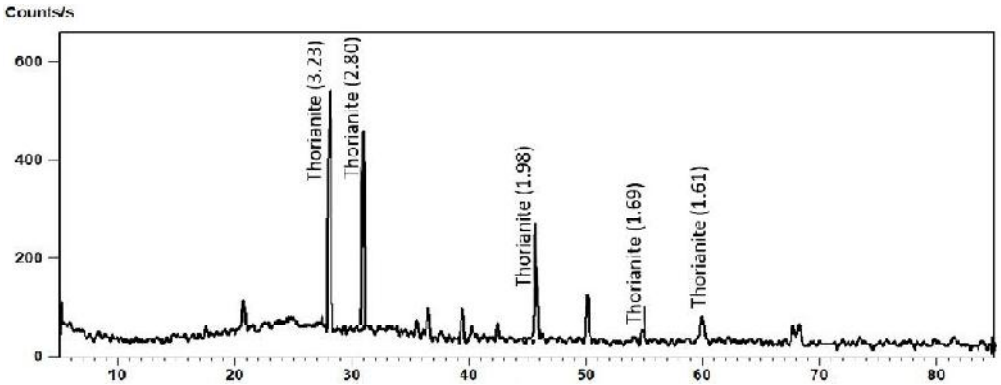

Fig. 28: XRD pattern of thorianite minerals ASTM card No. (4-556) of Gabal Suwair samples

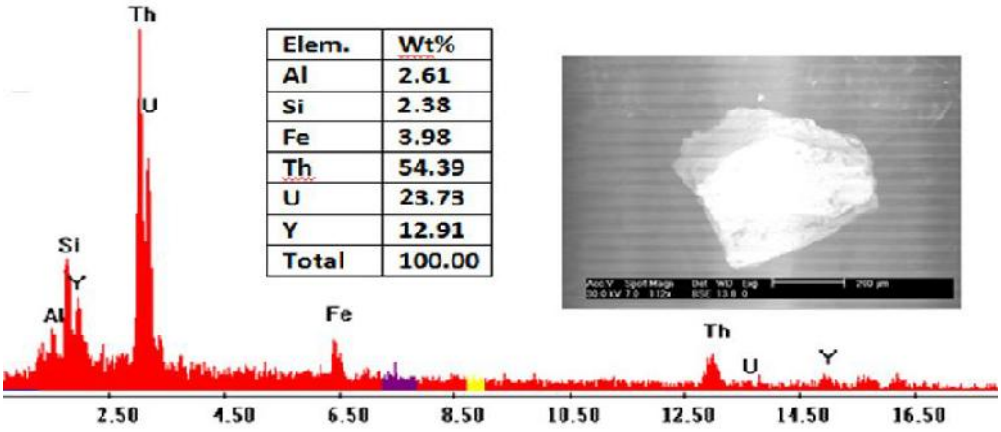

Elem.	Wt%
Al	2.61
Si	2.38
Fe	3.98
Th	54.39
U	23.73
Y	12.91
Total	100.00

Fig. 29: BSE and EDX analysis of thorianite minerals

solution. The SEM (EDX) analysis data of uranothorite shows that the Th, U, Si and Y are the main components (Fig. 30).

Niobium-tantalum minerals

Tanteuxenite-(Y):[(Y,Ca,Ce,U,Th)(Nb,Ta,Ti)$_2$O$_6$]

Euxenite-group minerals is a group of niobium-tantalum oxides that occur in Y, REE-rich pegmatites, with a formula AM_2O_6, where A site = Y, REE, U, and Th whereas M = Nb, Ti and Ta. Members of the euxenite group include euxenite-(Y), [Y(Nb,Ti)2O6], tanteuxenite-(Y), [Y(Ta,Ti,Nb)$_2$O$_6$], polycrase-(Y), [Y(Ti,Nb)$_2$O$_6$], and uranopolycrase, [UTi$_2$O$_6$] (Erict,2005). Euxenite group of minerals is similarly like aeschynite limited to pegmatites of euxenite subtype (Černý and Ercit 1989, 2005).

The tanteuxenite-(Y) mineral has been well identified from representative samples using XRD investigation after heating for 3 hours at 800^{o}C (Fig. 31), and accurate analysis by scanning electron microscope (ESEM). The investigated mineral crystals are dark brown to brownish black in color below the stereoscopic binocular microscope.

The obtained ESEM show that the grains

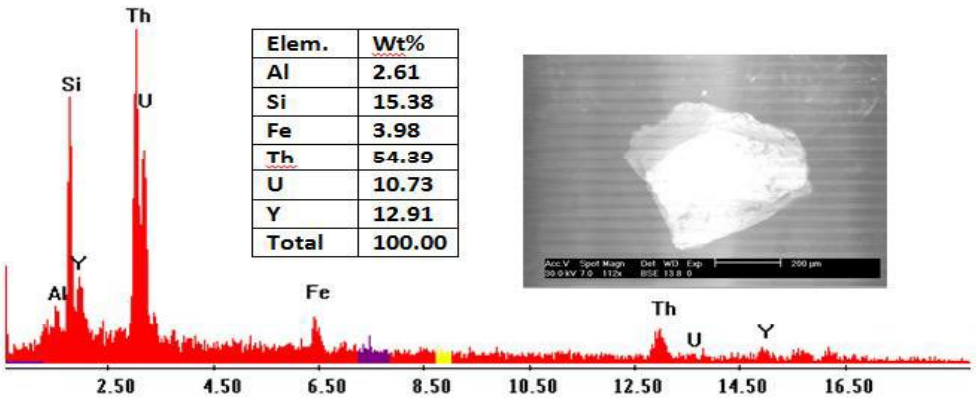

Elem.	Wt%
Al	2.61
Si	15.38
Fe	3.98
Th	54.39
U	10.73
Y	12.91
Total	100.00

Fig. 30: BSE image and EDX analysis of uranothorite of Gabal Suwair samples

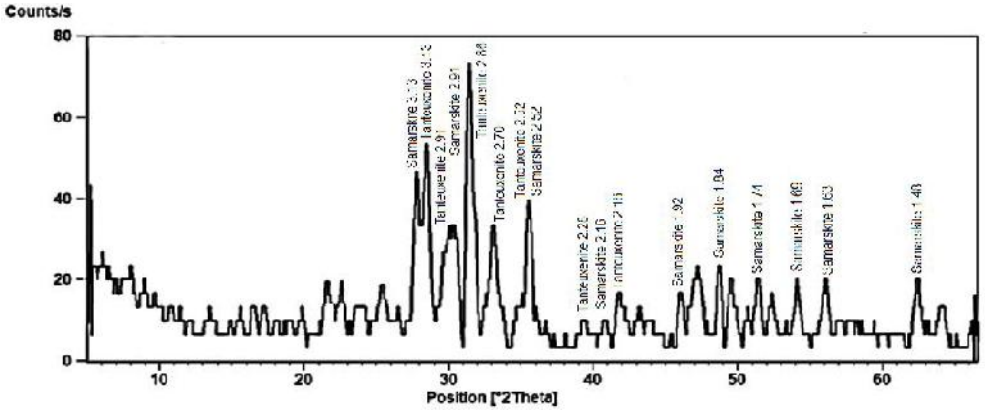

Fig. 31: X-ray diffractogram pattern of tanteuxenite ASTM card No. (31-1434) and samarskite minerals ASTM card No. (10-0398) of Gabal Suwair pegmatite

are enriched in uranium, titanium, yttrium and niobium (Fig. 32).

Samarskite (Y, Er)(Nb, Ta)$_2$O$_6$

Samarskite occurs as elongated crystals associated with tanteuxenite. The general structural formula of samarskite group of minerals is ABO_4 (Ercit, 2005), position A is occupied by Th, U, Y, Mn, Ca, Pb, REE, Na, Fe^{2+} and position B is occupied by Nb, Ta, Ti, Zr, Al, Fe^{3+} (Lumpkin and Ewing 1995). Samarskite mineral was identified using XRD investigation after heating and associated with tanteuxenite (Fig. 31). Anhedral to subhedral granular form of samarskite were detected in Gabal Suwair pegmatite. Most of samarskite grains have a characteristic resinous luster, translucent, compact, metamict and hard. The samarskite crystals are mainly dark yellowish brown in color. The semi-quantitative chemical composition of samarskite grains using scanning electron microscope (Fig. 33) revealed that enrichment in niobium, tantalum, yttrium and REE.

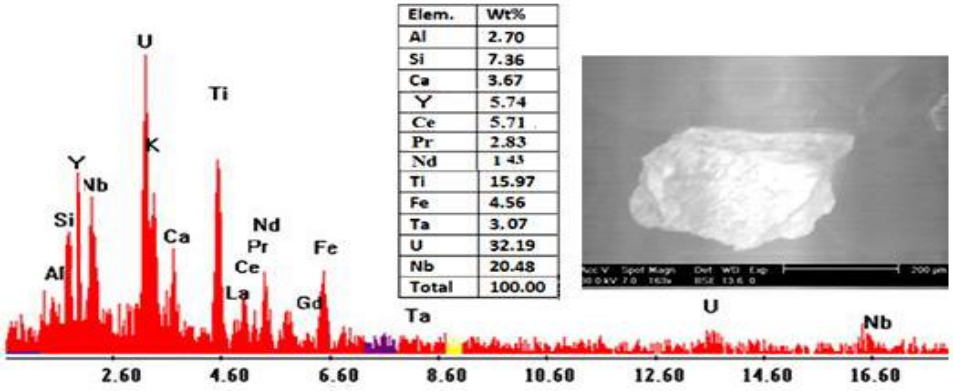

Fig. 32: BSE image and EDX analysis of tanteuxenite mineral of Gabal Suwair pegmatite samples

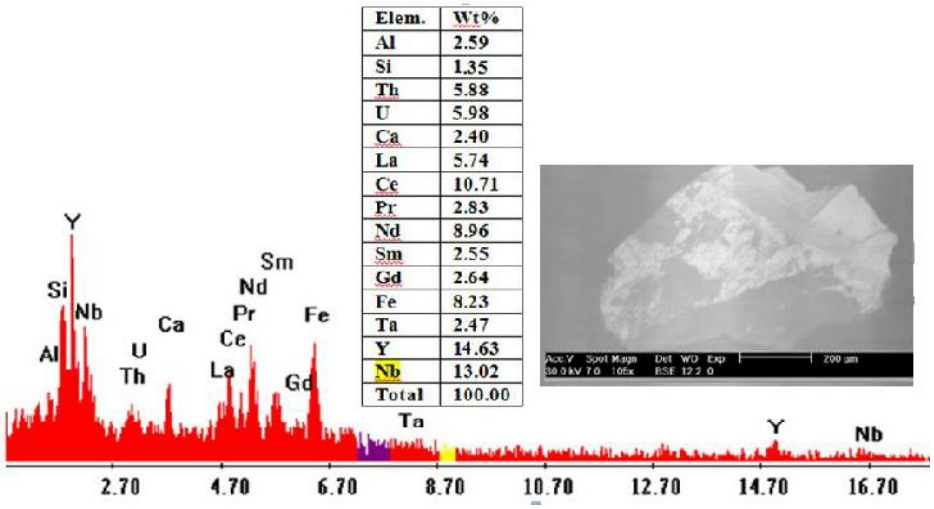

Fig. 33: BSE image and EDX analysis of samarskite mineral of Gabal Suwair pegmatite samples

Betafite (Ca, Na, U) (Ti, Nb, Ta)$_2$O$_6$ (OH).

Several minerals of the pyrochlore group, which includes betafites and microlites, often contain significant quantities of uranium along with rare-earth elements [Smith 1984]. The pyrochlore minerals are usually associated with rare-earth pegmatite or as accessory minerals in granitic rocks. Pyrochlore group is classified into three subgroups where pyrochlore mineral is the Nb-dominant member, microlite is the Ta-dominant member and betafite has 2Ti > (Nb+Ta) [Hogarth, 1977].

The studied betafite minerals in Khosh Daba pegmatites have dark brown to black color and adamantine luster. The picked

betafite crystals were detected by separate XRD pattern (Fig.34) after heated process as betafite specimens occur in the metamict state. EDX data revealed that the analysed betafite (Fig. 35) presents as inclusions contains differential concentrations of niobium, titanium, uranium and tantalum with appreciable amount of Fe, Y, REE and Al. The average of Ti attains 17.18% that is much higher than the average of Ta (5.5%) and the average of Nb attains 24.8%.

Accessory Minerals

Zircon and apatite

Zircon ($ZrSiO_{4)}$ appears in most separated samples as colorless, whitish brown and reddish brown color. Zircon crystals show adamantine luster in granitic samples, while, in radioactive samples metamictzircon have reddish resinous luster. ESEM investigation technique show certain inclusions of apatite [$(Ca_{10}(PO_4)_6(OH)_2$] are detected on the surfaces of zircon crystals and appearance as simultaneous over growths (Fig.36), that proposes that zircon postdates apatite in the studied granitic rocks.

Other zircon crystals have uranothorite inclusions or overgrowths (Fig.37). Thus, zircons with inclusions are interpreted as hydrothermal zircons, whereas inclusion-free zircons probably have a magmatic origin (Pelleter et al., 2007). That agrees with the direct crystallization by zircon-saturated fluids (Hoskin, 2005).

The changes in color from pale brown to reddish brown in different zircon samples are probably due to progressively higher uranium and thorium contents associated with each other that led to the metamictization on zircon crystals lattice. Claus (1936) has found that there are two types of brown or opaque zircons: 1) altered zircons with dull luster and frequently with rounded outlines, and 2) metamict zircons, with bright luster and sharply euhedral outlines. The studied metamict zircon crystals associated with uranium minerals attain brown and reddish brown color with euhedral crystals and adamantine luster. Metamict zircon has examined using scanning electron microscope, which shows relatively variable elemental composition, it is possible that such deficits are due to Th, and U elements replacing Zr (Fig. 37).

Copper mineralization

The Cu-minerals (atacamite, malachite and chalcocite) have been detected as fissure filling along the hydrothermal alteration zones and quartz stockworks, which occur mainly through the shear zone and fractures fillings of Gabal Khosh Daba area.

The Cu-minerals investigations of granite samples display low Cu-minerals content, while the sheared rocks have reformed Cu contents. Copper in the studied samples occurs mainly related to Gabal Khosh Daba area and less detected in Gabal Suwair area.

Atacamite($Cu_2Cl(OH)_3$)

Atacamite is occurs as small aggregates as cavity and fissure filling. It is reflected as the highest minerals associated with uranium minerals and hematite. The atacamite has green color and transparent to translucent crystal and acicular characters. Atacamite mineral has been identified using XRD investigation and the ESEM with EDX analysis (Figs. 38 and 39).

Malachite ($Cu_2CO_3(OH)_2$)

Malachite occurs as staining through the shear zone and fractures fillings, also present as scattered grains in the stockworks as green to blue color and dull luster. The ESEM with EDX results are shown on Fig.(40).

Chalcocite (Cu_2S)

It shows dark green color and generally very common in the studied uraniferous samples of Gabal Khosh Daba area. Chalcocite is associated with other copper minerals and could be used as a pathfinder element for uranium increases in the study area. The ESEM with EDX results of chalcocite mineral are shown on Fig.(41).

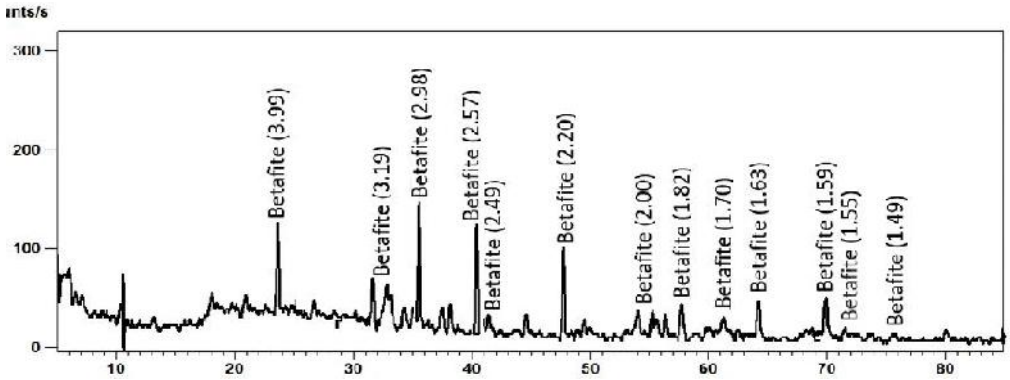

Fig. 34: XRD pattern of betafite minerals ASTM card No. (13-197) of Gabal Khosh Daba pegmatite

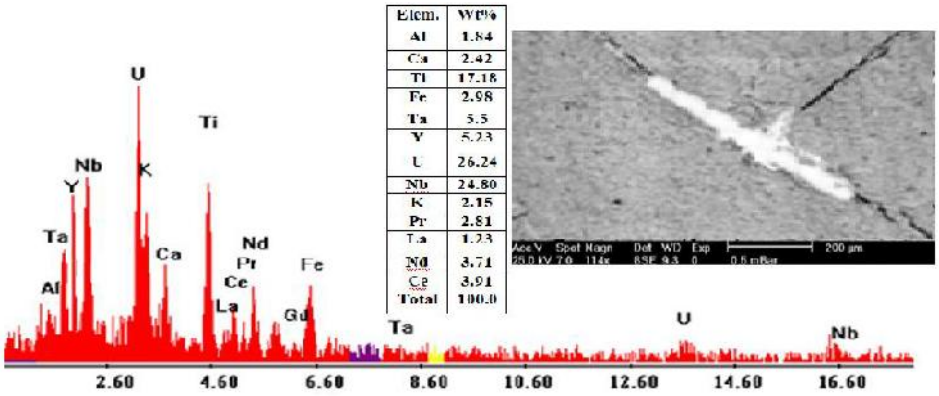

Fig. 35: BSE image and EDX analysis of betafite mineral appear as veins by very bright color of Gabal Khosh Daba pegmatite

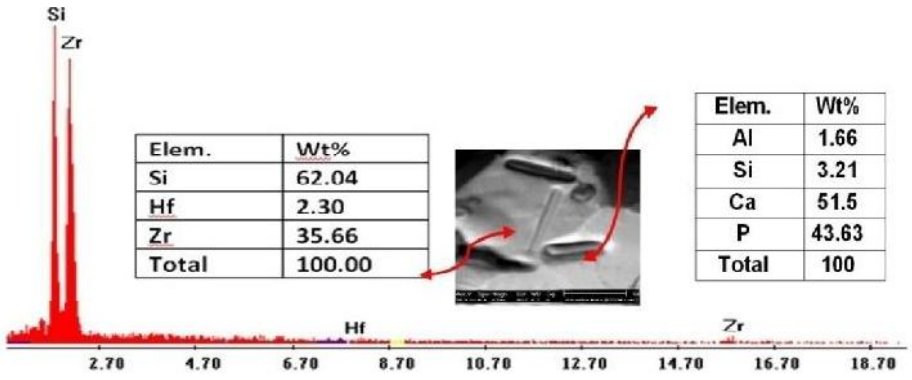

Fig. 36: BSE image and EDX of zircon contain apatite inclusion

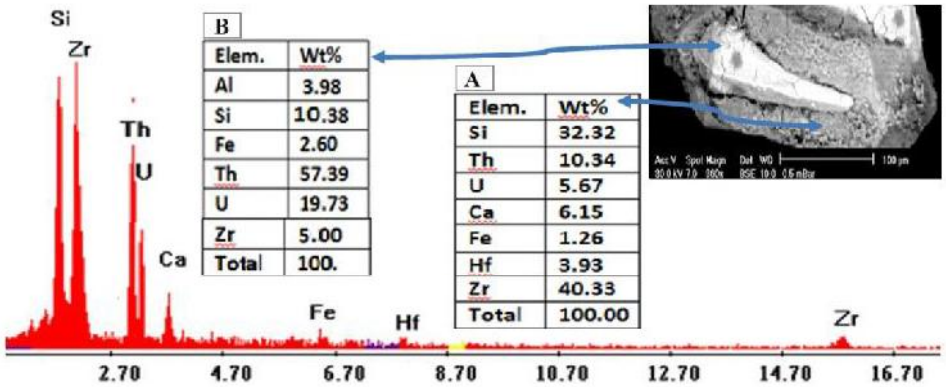

Fig. 37: BSE image and EDX of (A) Zircon (the host crystal) (B) uranothorite and zircon phase of Gabal Suwair samples

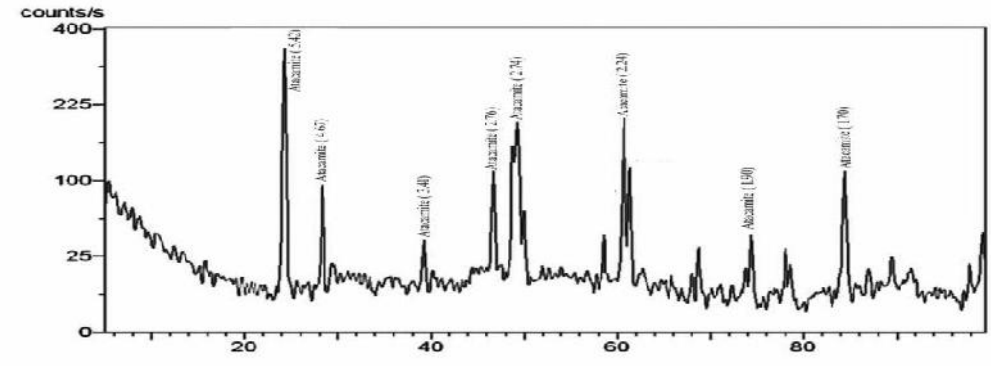

Fig. 38: XRD pattern of atacamite minerals of Gabal Khosh Daba

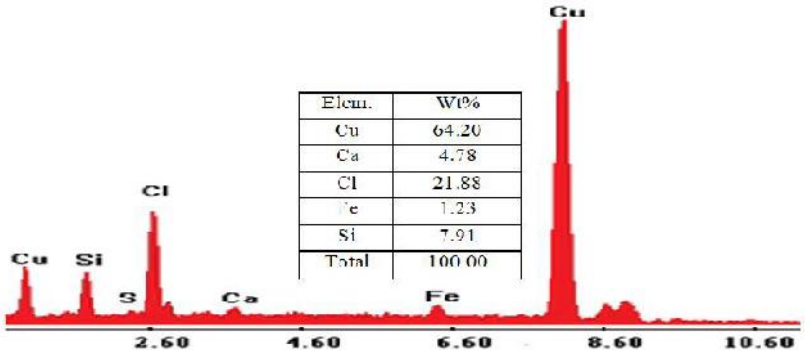

Fig. 39: EDX analysis of atacamite minerals

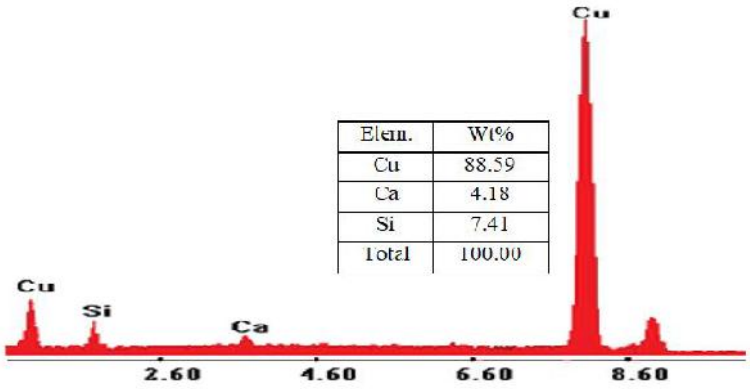

Fig. 40: EDX analysis of malachite minerals

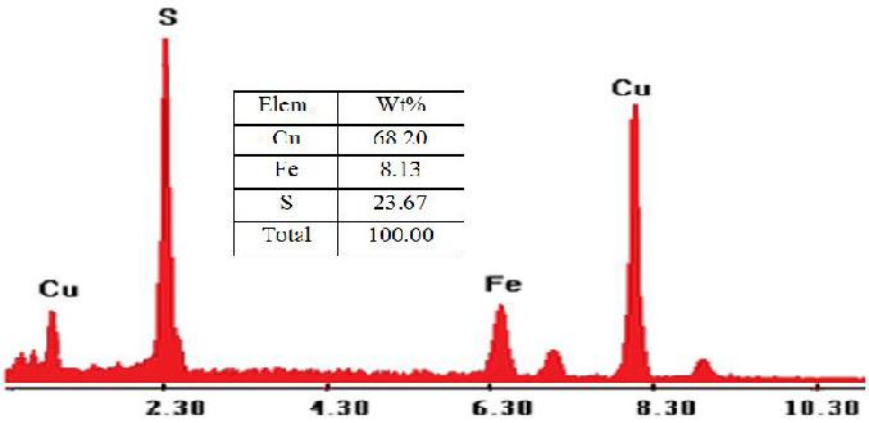

Fig. 41: EDX analysis of chalcocite minerals

CONCLUSIONS

The unzoned pegmatite of Gabal Suwair hosted in syenogranite and dissected by numerous fractures completely stained by iron oxides and associated with radioactive minerals, while, zoned pegmatite of Gabal Khosh Daba area hosted by monzogranite.

Most pegmatite bodies are varying in shape from linear or dykes like, tabular and uniform oval-shaped bodies. It is worth noting that Cerny (1991a,b) considered tabular pegmatites ranging from flat-lying to shallow dipping to be the most fractionated and best mineralized.

Zonation in pegmatite at Gabal Khosh Daba is display three internal zones including the wall zone, intermediate zone and core zone. Through the intermediate zone of pegmatites may include many distinct mineralized uraniferous zones. While, unzoned pegmatites show only a partial quantity, or even none, of mineral assemblage. However, the more

uranium-rich pegmatites display regular or typical zoning. Mineral assemblages of zoned pegmatites are normally related to fissures in the intermediate zone, as is the case in the Wodgina ore body in the Pilbara (Sweetapple et al., 2001b).

The radiometric studies of the anomalous pegmatite samples show that their equivalent uranium contents (eU) up to 670 ppm while their equivalent thorium contents (eTh) 180 ppm in Gabal Khosh Daba and display 520 ppm (eU) and 330 ppm (eTh) in Gabal Suwair.

Pegmatite bodies containing the uranium, thorium and niobium-tantalum minerals; these minerals include uraninite, brannerite, carnotite, uranothorite, thorianite, tanteuxenite, samarskite, and betafite discrete large crystals in zoned and unzoned pegmatite.

Mineralization in the intermediate zone that contain uranium and related minerals is greatly found include exceeds of niobium, tantalum and REE in the same mineral as assemblage in these zones.

The observed unzoned pegmatites are present as vein -like bodies or pocket-shape and well noticed thing is that the average eU/ eTh ratio is 1.7 in unzoned pegmatite, which means a secondary enrichment of uranium over thorium. The high eU/eTh ratio is due to the presence of uranium bearing accessories carried by hydrothermal solutions from the relatively deep-seated and were precipitated along fissures and fault plans within the pegmatites. While the presence of uranium minerals as discrete large crystals in zoned pegmatite shows that these minerals related to magmatic processes.

Thus, the studied mineralized zoned and unzoned pegmatites can be considered as a promising area for subsurface uranium exploration and required to understand and follow-up the system and sitting of the uranium mineralization in subsurface of this area by additional and advanced technical applications.

The high eU/eTh ratio is due to the presence of uranium bearing accessories carried by hydrothermal solutions from the relatively deep-seated and were precipitated along fissures and fault plans within the pegmatites. While the presence of uranium minerals as discrete large crystals in zoned pegmatite shows that these minerals related to magmatic processes.

Thus, the studied mineralized zoned and unzoned pegmatites can be considered as a promising area foe subsurface uranium exploration and required to understand and follow-up the system and sitting of the uranium mineralization in subsurface of this area by additional and advanced technical applications

REFERENCES

Abdalla, H.M.; Helba, H.A., and Mohamed, F.H., 1998. Chemistry of columbite-tantalite minerals in rare metal granitoids, Eastern Desert, Egypt. Mineralogical Magazine, 62, 821-836.

Akaad, M.K., and Noweir, A.M., 1980. Geology and lithostratigraphy of the Arabian Desert Orogenic belt of Egypt between Latitudes 25º 35' and 26º 30' N. Bull. Instit. Applied Geol., Jeddah, 4, 127-134.

Ali, M.A.; Abd El Gawad, A.E., and Ghoneim, M.M., 2021. Geology and mineral chemistry of uranium and thorium bearing minerals in Rare-metal (NYF) Pegmatites of Um Solimate, South Eastern Desert of Egypt. Acta Geologica Sinica. Accepted articles, htts://doi.org/10.111/1755, 6724-14708.

Barron, T., 1907. The Topography and Geology of The Peninsula of Sinai (Western Portion). Surv. Dept., Cairo, Egypt, 241p.

Bishr, A.H., 2007. Factors controlling mineralization of some shear zones in granites, South Sinai, Egypt. Ph.D. Thesis, Fac. Sci. Zagazig Univ., Egypt.

Cerny, P., 1991a. Fertile granites of Precambrian rare-element pegmatite fields: Is geochemistry controlled by tectonic setting or source lithologies? Precamb. Res. 51, 429-468.

Cerny, P., 1991b. Rare-element granitic pegmatites. I. Anatomy and internal evolution of pegmatite

deposits. Geosci. Can., 18, 49-67.

Cerny, P., and Ercit, T.S., 1989. Mineralogy of Niobium and Tantalum: Crystal Chemical Relationships, Pagarenetic Aspects and Their Economic Implications, In: Lanthanides, Tantalum and Niobium (Möler, P.; Černý, P., and Saupé, F.,Eds.),27-79.

Cerny, P., and Ecrit, T.S., 2005. The classification of granitic pegmatites revisited. The Canadian Mineralogist. 43, 2005-2026.

Claus, A., 1936. Zircons in rocks II. Igneous rocks. Am. J. Sci., 254, 521-554.

El-Gaby, S., 1975. Petrochemistry and geochemistry of some granites from Egypt. N. Jb. Miner. Abh., 124, 147-189.

El-Gaby, S.; List, F.K., and Tehrani, R., 1988. Geology evolution and metallogenesis of the Pan-Africa belt in Egypt, In: The Pan-African belt of the northeast Africa and adjacent areas(El-Gaby, S. and Greiling, R.O.,Eds). Viewing Berlin, 17-70.

El-Ghawaby, M.A., 1984. Image linear analytical approach to copper mineral exploration in South Sinai, Egypt. Inter. Atomic Energy Agency, United Nation Educational Scientific and Cultural Organization.

El-Ramly, M.F., and Akaad, M.K., 1960. The basement complex in the Central Eastern Desert of Egypt between latitudes 24° 30' and 25° 40', N. Geol. Surv. Egypt, paper 8, 35p.

El-Shazly, E.M., 1964. On the classification of the Precambrian and other rocks of magmatic Affiliation in Egypt. The 22nd Int. Geol. Cong., India, Sect. 10, 394.

El-Shazly, E.M.; Abdel-Hady, M.A.; El-Ghawaby, M.A.; El-Kassas, I.A., and El-Shazly, M.M., 1974. Geology of Sinai Peninsula from ERTS Satellite images. Remote Sensing Research Projects, Academy of Scientific Research and Technology, Cairo, Egypt.

El-Sheshtawy, Y.A., 1984. Petrographical and geochemical studies of granitic rocks around Wadi El-Sheikh, southwest Sinai, Egypt. Ph.D. Thesis, Al-Azhar Univ., Cairo, Egypt. 213 p.

Ercit, T.S., 2005. Identification and alteration trends of granitic-pegmatite-hosted (Y, REE, U, Th)–(Nb, Ta, Ti) oxide minerals: a statistical approach. Canadian Mineralogist. 43(4), 1291–1303.

Eyal, M., 1975. Stages in the magmatic history of the Precambrian in Sinai and Southern Negev. Ph. D. Thesis, Hebrew Univ., 117p.

Gaafar I.M.; Ali, K.G., and Meira M.I., 2014. Integration of airborne and carborne gamma-ray spectrometric surveys, Wadi El Gidami area, Central Eastern Desert, Egypt. Geophys. Soc. J., 12, 65-78.

Hogarth, D.D., 1977. Classification and nomenclature of the pyrochlore group. Am. Miner., 62, 403-10.

Hoskin, P.W.O., 2005. Trace-element composition of hydrothermal zircon and the alteration of Hadean zircon from the Jack Hills, Australia. Geochim.etCosmochim. Acta. 69, 637–648

Hume, W.F., 1935. Geology of Egypt. Part II: Volume II: The Fundamental Pre-Cambrian Rocks of Egypt and the Sudan; Their Distribution, Age and Character. Egypt. Geol. Survey, Cairo.

Hussein, A.A.; Ali, M.M., and El-Ramly, M.F., 1982. A proposed new classification of the granites of Egypt. J. Volc. Geoth. Res., 14, 187-198.

Ibrahim, M.E., 1991. Geology and radioactivity of Wadi Zaghra area, South central Sinai, Egypt. Ph.D. Thesis, Mansoura Univ., Egypt, 181p.

Lumpkin, G.R., and Ewing, R.C., 1995. Geochemical alteration of pyrochlore group minerals: Pyrochlore subgroup. American Mineralogist, 80, 732–743.

Matsubara, S.; Kato, A., and Matsuyama, F., 1995. Nb-Ta minerals in a lithium pegmatite from Myokenzen, Ibaraki Prefecture, Japan. Mineralogical J., 17, 338-345.

Mock, R.L., and Ohmoto, H., 1997. Nondetrital Origins of Uranium-bearing Minerals and Pyrites in Early Proterozoic Quartz-Pebble Conglomerates of the Elliot Lake District, Ontario. 7th Annual V. M. Goldschmidt Conf., 2273p.

Pabst, A., 1952. The metamict state. The Amer. Mineral., 37, 137-157.

Pal, D.C.; Mishra, B., and Bernhardt, H.J., 2007. Mineralogy and geochemistry of pegmatite hosted Sn-, Ta–Nb-, and Zr–Hf-bearing minerals from the southeastern part of the Bastar-Malkangiri pegmatite belt, Central

India. Ore Geol. Rev., 30, 30-55.

Pelleter, E.; Cheilletz A.; Gasquet D.; Mouttaqi A.; Annich M.; El Hakour A.; Deloule T., and Féraud G., 2007. Hydrothermal zircons: A tool for ion microprobe U–Pb dating of gold mineralization (Tamlalt–Menhouhou gold deposit-Morocco). Chem. Geol., 245, 135-161.

Raslan, M.F., 2015. Occurrence of Samarskite-Y in the Mineralized Umm Lassifa Pegmatite, Central Eastern Desert, Egypt. Geologija, 58(2), 213-220.

Raslan, M.F., and Ali, M.A., 2011. Mineralogy and mineral chemistry of rare-metal pegmatites at Abu Rusheid granitic gneisses, South Eastern Desert, Egypt. Geologija, 54(2), 205–222, Ljubljana, http://dx.doi.org/10.5474/geologija.2011.016.

Sallam, O.R.; Al Shami, A.S.; Abbas, A.A., 2019. Geology and mineralogy of a radioactive pegmatite body at WadiZaghra area, southeastern Sinai, Egypt. Nucl. Sci. Scient. J. 8A, 191- 205.

Schwartz, M.O., 1992. Geochemical criteria for distinguishing magmatic and metasomatic albite enrichment in granitoids: Examples from the Ta-Li granite Yichun (China) and the Sn-W deposits Tikus (Indonesia). Mineralium Deposita, 27, 101-108.

Smith, D.K., 1984. Uranium mineralogy, In: Uranium geochemistry, mineralogy, geology, exploration and resources(de Vivo F. et al.). IMM, London, 43-88.

Streckeisen, A.L., 1976. To each plutonic rocks its proper name. Earth Sci, Rev., 12, 1-15.

Sweetapple, M.T.; Cornelius, H., and Collins, P.L.F., 2001b. Tantalum mineralization of the Wodgina pegmatite district: the Wodgina and Mt. Cassiterite pegmatite orebodies. Metallogenesis of the North Pilbara granite-greenstones, Western Australia-A field guide. Geol. Surv. West Aust Rec. 11, 41-58.

Ulvsand, T.; Finck, R.R., and Lauritzen, B., 2002. Barents Rescue 2001 LIVEX. NKS-54, ISBN. 87-7893-108-8.

Ulvsand, T., Finck, R.R., Lauritzen, B., 2002.
Barents Rescue 2001
LIVEX. NKS-54, ISBN: 87-7893-108-8.

William, S.B.; Hanson, S.L., and Falster, A.U., 2006. Samarskite-Yb: A new species of the samarskite group from the Little Pasty pegmatites, Jefferson County, Colorado. Canadian Mineralogist, 44(5), 1119-1125.

دراسات جيولوجية ومعدنية للبجماتيت الحامل لليورانيوم والثوريوم بمنطقة جبل صوير وجبل خوش دابا، سانت كاترين، جنوب وسط سيناء، مصر

محمود مصيلحى نصر

تتواجد صخور البجماتيت شمال مدينة سانت كاترين بجنوب وسط سيناء بمنطقة جبل صوير وجبل خوش دابا، حيث تغطى المنطقة صخور الدرع العربى من الجرانيت القديم (الجرانوديوريت) والجرانيت الحديث (مونزوجرانيت وسيانوجرانيت) وتعتبر صخور البجماتيت المتواجدة مع المونزوجرانيت والسيانوجرانيت هى أحدث صخور الدرع العربي بالمنطقة. وتسجل صخور البجماتيت العديد من الشاذات الإشعاعية فى كلا النوعين سواء البجماتيت النطاقى بجبل خوش دابا او البيجماتيت الغير نطاقى بجبل صوير. ولقد سجلت القياسات الإشعاعية قيم لمكافئ اليورانيوم تصل الى ٦٧٠ جزء فى المليون بالبجماتيت النطاقى المتواجد بجبل خوش دابا بينما سجلت القياسات قيم تصل الى ٥٢٠ جزء فى المليون لمكافئ اليورانيوم بصخور البجماتيت الغير نطاقى بجبل صوير. أما الثوريوم فقد سجلت القياسات الإشعاعية قيم ١٨٠ جزء فى المليون بصخور البجماتيت بجبل خوش دابا بينما سجلت ٣٣٠ جزء بالمليون بصخور البجماتيت بجبل الصوير.

كشفت الدراسات المعدنية عن وجود معادن اليورانيوم (مثل اليورانينيت، البرانيريت والكارنوتيت) على شكل بلورات منفصلة فى البجماتيت النطاقى بجبل خوش دابا، فى حين أن صخور البجماتيت الغير نطاقى تحتوى على معادن النوبيم-تانتالم ومعادن اليورانوثوريت والثوريوم (مثل السامرسكيت، البيتافيت، التانتكسونيت، اليورانوثوريت والثوريت).

يشير وجود معادن اليورانيوم الأولية فى البجماتيت النطاقى الى ان المعادن المشعة تكونت اثناء تكوين صخور البجماتيت من الماجما الغنية بعناصر اليورانيوم، فى حين ان وجود معادن اليورانيوم الثانوية فى شقوق وفجوات البجماتيت الغير نطاقى يدل على الارجح بأن مصدر التمعدنات بهذه الصخور يرجع الى المحاليل الحارمائية الغنية بعنصري اليورانيوم والثوريوم.

ويتضح من الدراسة ان البجماتيت بمنطقة سانت كاترين (جبل صوير وجبل خوش دابا) يعتبر ذو اهمية إقتصادية حيث انه مصدر للمواد المشعة (اليورانيوم والثوريوم)، وتوصى الدراسة بمزيد من أعمال التنقيب عن التمعدنات تحت السطح من خلال تقنيات متقدمة للعمل على تتبع وتنمية وتقييم الخامات المتواجدة بالمنطقة.